Zircaloy-4 cladding hydride reorientation under ring compression test conditions

Vincent Busser, Jean Desquines, Christian Duriez, Marie-Christine Baietto, Jean-Paul Mardon

Zircaloy-4 cladding hydride reorientation under ring compression test conditions

V. BUSSER, J. DESQUINES, C. DURIEZ
Institut de Radioprotection et de Sûreté Nucléaire (IRSN), Direction de Prévention des Accidents Majeurs, Centre d'Etudes de Cadarache, BP3, F-13115 Saint-Paul lez Durance Cedex (France)
Tel: 33 4 42 19 94 90 , Fax: 33 4 42 19 91 66, Email: vincent.busser@irsn.fr

M.C. BAIETTO-DUBOURG
Université de Lyon, CNRS, INSA-Lyon, LaMCoS UMR5259, F-69621 Villeurbanne Cedex (France)

J.P. MARDON
AREVA-NP SAS, 10 rue Juliette Récamier, F-69456 Lyon Cedex 06 (France)

Abstract – *Temperature increase induces partial or total dissolution of Zirconium hydrides. After this dissolution phase, a cool down under applied stresses can promote radial precipitation of hydrides. Radial hydrides are known to have a deleterious impact on the cladding strength and ductility. The objective of this study is to evaluate, using ring compression tests (RCT), the required stress level leading to the formation of radial hydrides within the cladding during a thermal-mechanical transient. The obtained results are in good agreement with literature data obtained using different specimen geometry. The tests provide quantitative information on the radial hydride induced embrittlement. Ring compression test appears to be an efficient tool for hydride reorientation analysis.*

I. INTRODUCTION

The French "Institut de Radioprotection et de Sûreté Nucléaire" (IRSN) is involved in research activities addressing the main safety issues. The radial hydride precipitation in zirconium cladding alloys has potentially a deleterious impact on cladding integrity. It is thus of primary interest for IRSN to determine the key parameters controlling radial hydride precipitation.

Under normal PWR operating conditions, the cladding is oxidized by the water, leading to the formation of an oxide layer on the external surface. This oxidation process also induces hydrogen diffusion towards the cladding [1]. When exceeding the hydrogen solubility limit in the zirconium alloy matrix, hydride platelets precipitate [2]. After PWR irradiation, mainly circumferentially-oriented hydrides are observed in Stress Relieved Annealed (SRA) Zircaloy 4 [3].

Depending on the hydrogen content, temperature increase induces partial or total dissolution of these hydrides [4]. After this heating phase, a cool down under applied stresses can promote radial precipitation of hydrides [5]. These radial hydrides have potentially a deleterious impact on the cladding strength and ductility [6].

Hydride reorientation tests are usually performed on pressurized tubes. This technique requires a test at each stress level tested and thus induces significant material consumption. Recently, hoop tensile tests with gage section, loaded with inserted mandrels, enabled the determination of the influence of a wide range of stresses on hydride reorientation using a single specimen [7]. But these tests are affected by mandrel-sample friction, that is not accurately quantified and subjected to variations. On the opposite, ring compression test is not influenced by friction occurring at the contact interface between the sample and the loading device as it is of a rolling type [8-9].

The objectives of this study are: i) to evaluate the stress conditions leading to the formation of radial hydrides within the cladding during thermal-mechanical transient using ring compression tests (RCT), and ii) to examine the consequences on specimen embrittlement.

II. PRELIMINARY CALCULATIONS

Stress and strain fields used for hydride reorientation testing were numerically computed using the Finite Element Method (FEM). A hydride reorientation treatment is characterised by three steps: 1. the ring is heated to the specified maximum temperature, 2. the temperature being stabilized, the mechanical load is applied to the ring, 3. the ring is cooled down until room temperature.

The complex hoop stress (the hoop direction corresponds to the θ direction shown in Figure 1) response during a RCT to the thermal mechanical loading was obtained. Because the aim of the test is to use this hoop stress distribution to characterize radial hydride precipitation, it is necessary to keep the stress field constant during the entire thermal-mechanical loading. A strategy to obtain such a constant stress field was thus developed.

Since the ring sample is submitted to plane strain loading conditions [10], the calculations are conducted using two-dimensional approach. The ring mesh is constituted of 2160 4-node elements (linear interpolation). The ring material is supposed to behave isotropically and to be well modeled with elastic-plastic constitutive relations. The isotropic strain-hardening tensile law is a power-law : $\sigma = K\left(\varepsilon^{p}\right)^{n}$, where σ and ε^{p} are the equivalent Von-Mises stress and the corresponding equivalent plastic strain respectively, and K and n are two material parameters determined in a previous study [10]. The mechanical properties of the ring and loading device are specified in Table I.

TABLE I

Mechanical properties of the ring sample and the loading device

	Ring	Load. device
Young Modulus (MPa)	116 116 – 59 T(K)	500 000
Poisson's ratio	0.325	0.325
Thermal exp. coeff. ($°C^{-1}$)	$5.62\ 10^{-6}$	
K	640	
n	0.03	

Many thermal transients have been modeled. The maximum temperature ranged between 20°C and 400°C. The predicted maximum hoop stress occurs at the equatorial location and at the outer diameter. It is labeled σ_A (see Fig. 1). The correlation between the numerical stress value σ_A (MPa) and the applied force F (N) is independent of the maximum temperature as long as the load is smaller than a critical value, here 30 N/mm (see Fig. 2). All the curves are superimposed whatever the temperatures considered up to a force equal to 30 N/mm.

$$\frac{F}{L} = 0.07489.\sigma_A - 1.405.10^{-5}.\sigma_A^2 \qquad (1)$$

where L is the ring axial length.

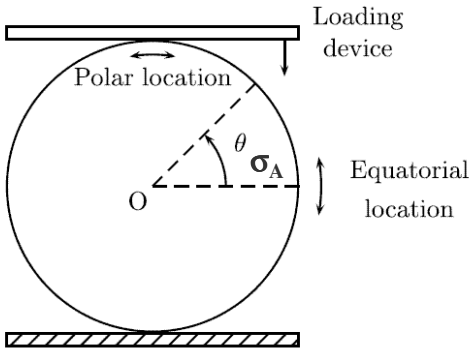

Fig. 1. Definition of the equatorial and polar ring locations (axial direction view) [10]

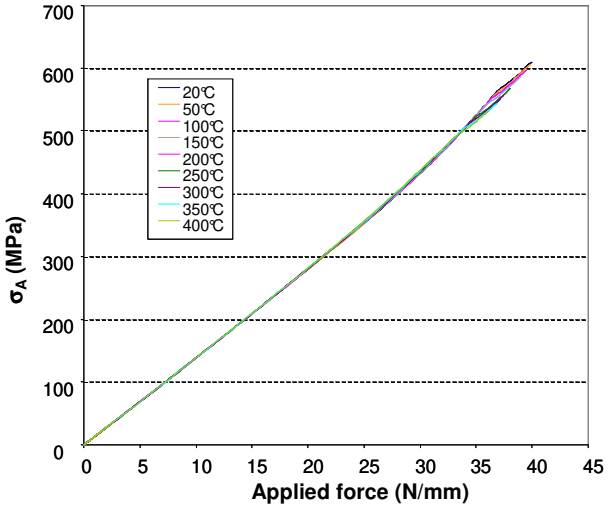

Fig. 2. Evolution of the maximum value σ_A of the hoop stress σθθ versus the applied force F

The outer diameter equatorial region of the ring is characterized by a tensile stress field. In the hoop direction, the tensile stress ranges between 0 up to the maximum stress σ_A.

III. EXPERIMENTAL PROCEDURE

1. Hydride reorientation treatment

Hydrided SRA Zircaloy-4 cladding segments have been prepared. The chemical composition of the alloy is mentioned in Table II.

TABLE II

Chemical composition of the alloy (in wt%)

	Sn	Fe	Cr	O
Low-tin SRA Zy-4	1.32	0.21	0.11	0.141

The tubes were loaded with gaseous hydrogen by AREVA at elevated temperature. It leads to uniform circumferentially-oriented hydride distribution. Two hydrogen contents were investigated, 100 and 500 wppm.

These tests were performed using a mechanical testing device INSTRON 5566 equipped with a heated chamber. Twenty-millimeter-long samples were used for hydride reorientation treatment. It induces stress gradients depending on both circumferential and radial locations in the ring. The loading conditions of the different tests performed are reported in table III.

TABLE III

Hydride reorientation test matrix

Sample I.D.	Heating rate (°C/min)	Tmax (°C)	Maximum stress σ_A (MPa)	Dwell time at Tmax (min)	Cooling rate (°C/min)
H100_04	5	342	229	100	0.4
H100_05	5	342	0	100	0.4
H500_01	5	344	225	180	0.4
H500_02	5	344	0	180	0.4

Two samples were tested simultaneously. The procedure was as follows: i) sample one: first the temperature is increased up to about 350°C with an heating rate of 5°C/min, secondly a dwell time is imposed, and thirdly the temperature is decreased with a controlled cooling rate down to room temperature (see Fig. 3) while a mechanical loading is simultaneously applied since the beginning of the test, ii) sample two charged with the same hydrogen content, called the reference sample, was submitted only to the same thermal transient (see Fig. 4).

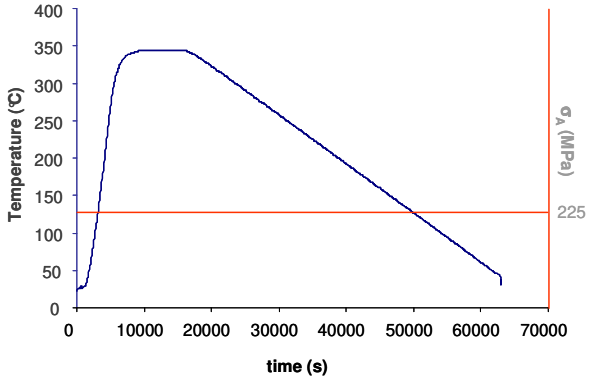

Fig. 3. Thermal-mechanical transient for specimens H100_04

The mechanical load is applied during temperature stabilizing and its is maintained during cooling down.

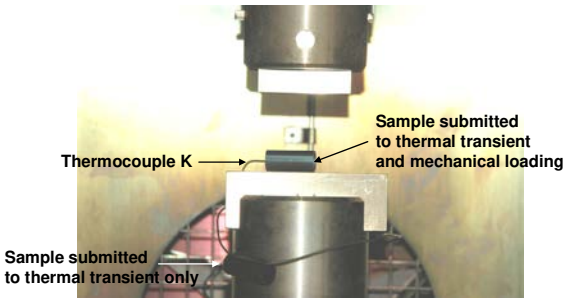

Fig. 4. Experimental device for reorientation tests

Finite-Element calculations provided a correlation between the maximum hoop stress level and the applied load (see Eq. 1 and Table IV). Under controlled loading conditions, the stress field in the cladding was demonstrated to be independent on cladding temperature. It means that, at a given location, hoop stress remains constant during the entire thermal-mechanical transient.

TABLE IV

Parameters of hydride reorientation test matrix

	Maximum stress (MPa)	Axial length of the ring (mm)	Calculated maximum applied load (N)
H100_04	229	23.3	382
H500_01	225	22.3	360

After the hydride reorientation test, each sample was then cut in two 10-mm-long rings. One was used for metallographic analysis, while the second was used to evaluate the loss of ductility induced by the precipitation of radial hydrides within the cladding.

2. Ring compression test after reorientation treatment

Ring compression tests were systematically performed at room temperature on 10-mm-long ring sample, previously submitted to a hydride reorientation treatment. Displacement-controlled tests were performed with a 1mm/min load line displacement rate. The ring orientation is the same as for hydride reorientation tests.

3. Metallographic analysis

Metallographic analysis was performed on the four tested samples. Cross sectional specimens were embedded in a resin and carefully prepared with an automatic grinding and polishing machine. The embedded samples were also chemically attacked with a solution of HNO_3, HF and water. They were observed with a LEICA optical microscope.

IV. RESULTS AND DISCUSSION

Metallographic analysis highlighted significant hydride reorientation in locations correlated to tangential tensile stress levels exceeding a threshold (see Fig. 5 and 6): the two preferred sites are situated at the outer equatorial surface and at the inner polar surface of the sample.

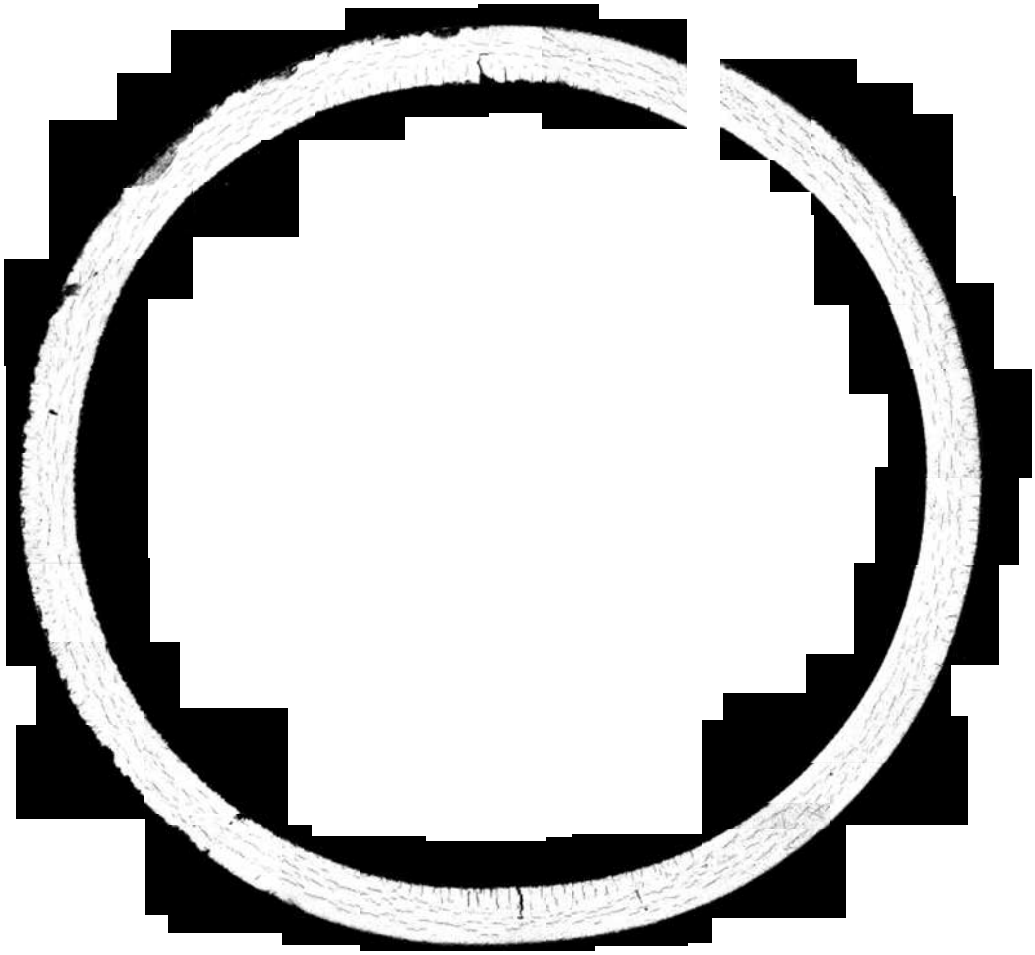

Fig. 5. Optical micrograph after a hydride reorientation test for the H100_04 specimen

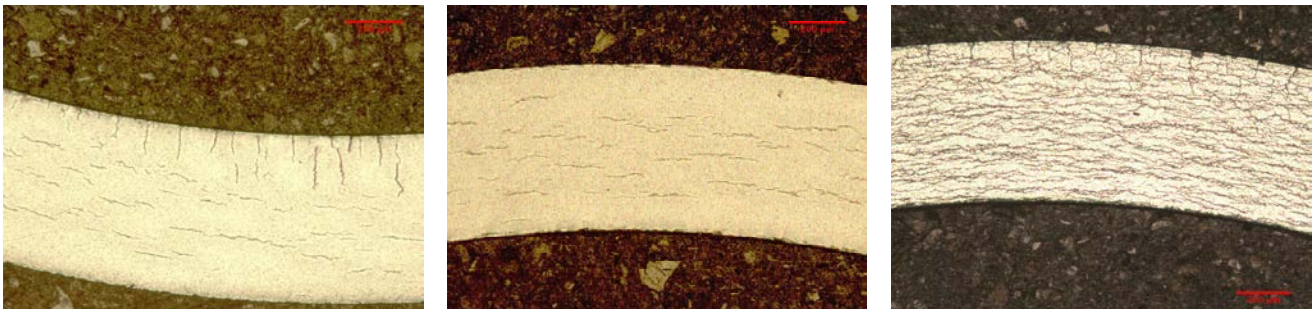

Fig. 6. Optical micrograph after a hydride reorientation test for the H100_04 (polar location), H100_05 (polar location), H500_1 (equatorial location) specimens (from left to right).

A methodology was developed in order to interpret the results of these tests. The aim being to assess in a good agreement the critical stress levels inducing radial hydride precipitation, an analytical evaluation of the stress distribution within the cladding was conducted.

Due to geometrical and loading symmetries, the modeling of the ring compression test can be reduced to one forth as shown in Fig. 7.

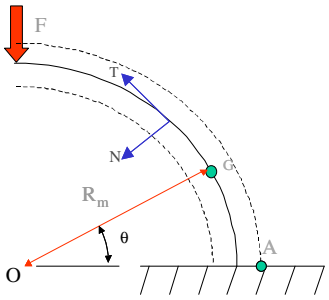

Fig. 7. Geometry of the problem

Under the thin shell assumption, the hoop stress $\sigma_{\theta\theta}$ can be calculated at any point G as a function of the applied load F.

$$\sigma_{\theta\theta}(r,\theta) = -\frac{6R_m F}{Le^3}\left(\frac{2}{\pi} - \cos\theta\right)(r - R_m) - \frac{F}{2Le}\cos\theta \qquad (2)$$

where R_m, L, e are respectively the average radius, the axial length and the thickness of the ring.

It is possible to normalize the tangential stress distribution using a shape function $f_{\theta\theta}$. $f_{\theta\theta}$ is the ratio of the tangential stress at any point and the maximum stress occurring at equatorial location, previously mentioned.

$$\sigma_{\theta\theta}(r,\theta) = \sigma_A . f_{\theta\theta}(r,\theta) \qquad (3)$$

Combining Eq. 2 and 3 leads to the shape function:

$$f_{\theta\theta} = \frac{\frac{3R_m}{e}\left(\frac{2}{\pi} - \cos\theta\right)\frac{2(r - R_m)}{e} + \frac{1}{2}\cos\theta}{\frac{3R_m}{e}\left(\frac{2}{\pi} - 1\right) + \frac{1}{2}} \qquad (4)$$

The metallographic data analysis for phenomena controlled by stress levels can be easily assessed using separately, on one side, a shape function threshold and, on the other side, a tangential stress value (σ_A) (see Fig. 8).

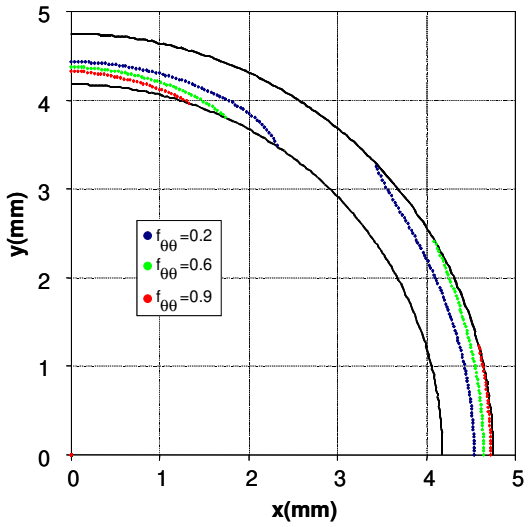

Fig. 8. $f_{\theta\theta}$ function mapping within the cladding

In the vicinity of the contact region between the loading device and the sample, the analytical assessment of stress distribution is far from accurate. Optical micrograph analysis was thus only performed in the region around the outer equatorial location. Many angular sectors (θ) were examined. For each angular sector studied on the micrographs, three regions are evidenced along the radial direction from the outer to the inner radius: 1. a region with only radial hydrides, 2. a region with mixed circumferential and radial hydrides, 3. a region with only circumferential hydrides, characterized by a maximum radius. The two thresholds defining the three zones allow the estimation of the 100% radial hydride threshold and the incipient radial hydride precipitation threshold (see Fig. 9).

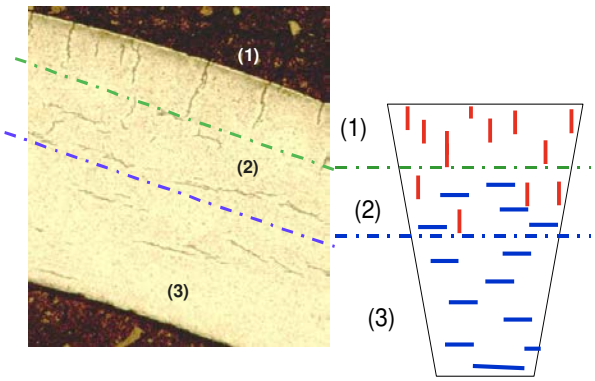

Fig. 9. Definition of both thresholds

Each optical analysis is localized by the polar coordinates s and r. s is the distance of the angular sector with respect to the equatorial location and r (comprised between inner radius and outer radius of the cladding) is the radius of the first radial hydride within the thickness e of the cladding.

The fraction X of the cladding thickness in which radial hydrides are observed is defined as:

$$X = \frac{R_{ext} - r}{e} \tag{5}$$

Considering Eq. 4 and 5 leads to:

$$X = \frac{1}{2} - \frac{1}{2}\frac{\left[\frac{3R_m}{e}\left(\frac{2}{\pi}-1\right)+\frac{1}{2}\right]f_{\theta\theta} - \frac{1}{2}\cos\left(\frac{s}{R_e}\right)}{\frac{3R_m}{e}\left(\frac{2}{\pi}-\cos\left(\frac{s}{R_e}\right)\right)} \tag{6}$$

For specimens with hydrogen content of 100ppm, there is a full dissolution of hydrides during the heating phase of the thermal transient and full hydrogen content precipitation during the cooling phase. It is also possible to observe the region 1 characterised by 100% radial hydrides (see Fig. 10). For the H500_01specimen, with 500 ppm, the results are different because circumferential hydrides are not entirely dissolved during the heating phase of the heat treatment (see Fig. 11). Some circumferential hydrides are still observed everywhere in the sample. Therefore, the specimen analysis with large hydride contents can be conducted only for two regions.

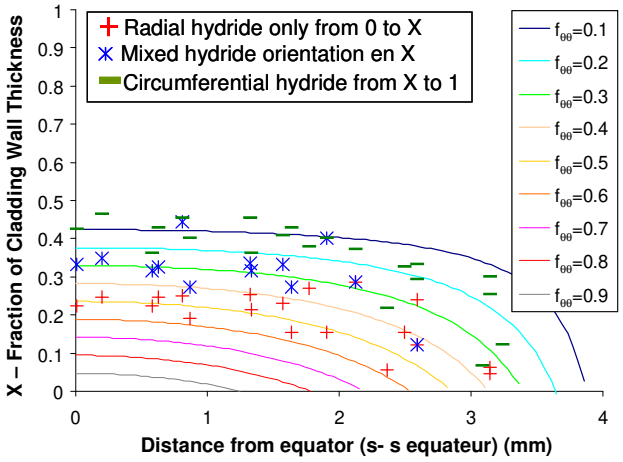

Fig. 10. Optical micrograph analysis of the H100_04 specimen

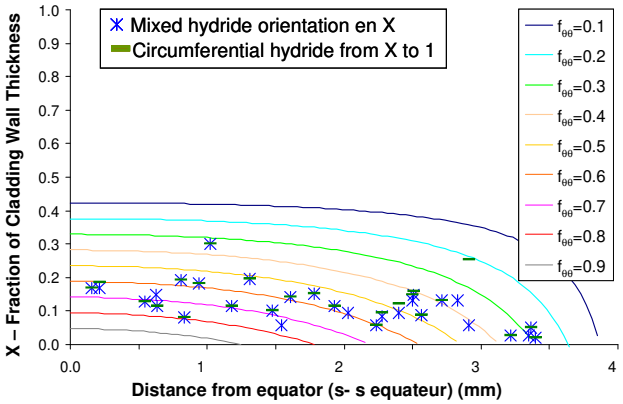

Fig. 11. Optical micrograph analysis of the H500_01 specimen

The stress field, determined by finite element calculations, is consistent with the observed distribution of hydrides over the entire sample cross-section. Two hoop stress thresholds are derived, for zero hydride reorientation and full radial hydride orientation. Fig 10 and 11 contribute to the threshold assessments. The results are summarized in Tables V and VI.

TABLE V

Stress threshold for incipient radial hydride precipitation

	Max. stress at equatorial location (MPa)	$f_{\theta\theta}$	Corresponding reorientation stress (MPa)
H100_04	229	0.27	62
H500_01	225	0.31	70

TABLE VI

Stress threshold inducing 100% radial hydride precipitation
(NA : Not available)

	Max. stress at equatorial location (MPa)	$f_{\theta\theta}$	Corresponding reorientation stress (MPa)
H100_04	229	0.42	96
H500_01	225	*NA*	*NA*

Hoop stress threshold for 0% radial hydride precipitation deduced from other specimen geometry are in general in the range of 70-120MPa for Zircaloy-4 alloys and for a maximum temperature of the thermal transient of about 400°C [7,11,12]. The threshold increasing with hydrogen content is consistent with literature results [4]. The value deduced from this study appears to be consistent with literature, perhaps a little bit lower than expected. However, a very low cooling rate was used here, promoting lower hydride reorientation thresholds [13].

After hydride reorientation treatment, samples were mechanically loaded using ring compression tests at room temperature in order to assess the influence of radial hydride precipitation on the sample ductility. The obtained load-displacement curves are illustrated in fig 12 (for 100 wppm hydride content) and 13 (for 500 wppm hydride content). The H100_04 specimen, with extended radial hydrides and no circumferential hydrides close to the outer diameter, has a significantly lower ductility than the H100_05 (without hydride reorientation). A similar result is observed on the 500 wppm samples. An outer diameter crack is nucleated at the most deformed locations. The failure load of a specimen with reoriented hydrides is 60% lower than the one of a specimen without radial hydrides. The figure 14 shows the crack pattern which can be easily linked to precipitated radial hydrides. These results are

consistent with similar mechanical tests performed on Zircaloy tubing with radial hydrides [7].

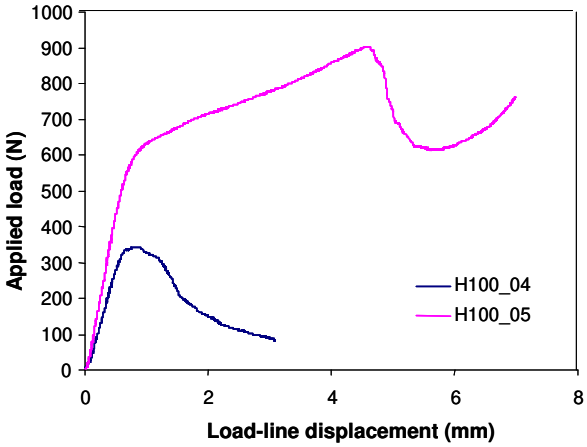

Fig. 12. Load-displacement curve of the specimen H100_04 and H100_05 submitted to a RCT at room temperature

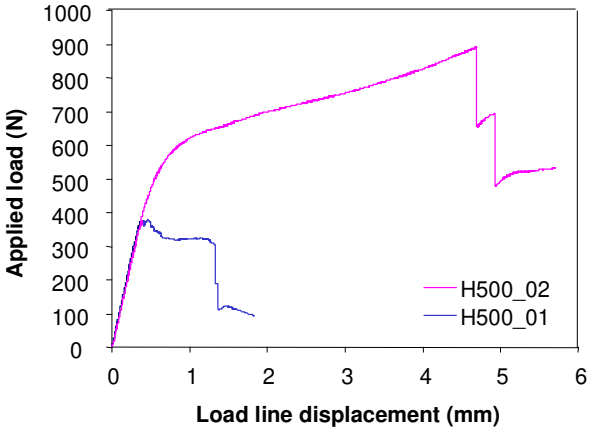

Fig. 13. Load-displacement curve of the specimen H500_01 and H500_02 submitted to a RCT at room temperature

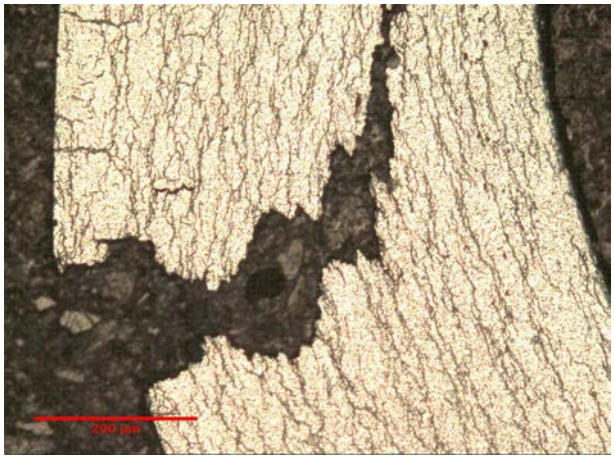

Fig. 14. Optical micrograph of the specimen H500_01 submitted to a ring compression test at room temperature after the reorientation treatment

VI. CONCLUSIONS

Ring compression test is an efficient tool to produce stress-controlled hydride reorientation in nuclear cladding. In this paper, analytical approach and numerical simulations, based on Finite Element Method, were performed to improve the understanding of the test.

Hydrided Zircaloy-4 (100 and 500ppm) were tested. The combined experimental-numerical analysis approach allowed for an assessment of a value of the stress threshold inducing radial precipitation of hydrides during a thermal transient. Criterion deduced from only two tests is not so far from the results presented in literature. Further modeling is required at polar locations.

Moreover, a ring compression test provides quantitative information on the radial hydride induced embrittlement. The results of the ring compression tests on samples with hydride reorientation using the RCT approach yielded embrittlement behavior consistent with literature data.

REFERENCES

1. C.E. ELLS, Hydride precipitates in zirconium alloys, *Journal of Nuclear Materials*, **vol. 28**, pp.129-151 (1968)

2. A. McMINN, E.C. DARBY, J.S. SCHOFIELD, *The thermal solubility of hydrogen in zirconium alloys, Zirconium in the Nuclear Industry, ASTM STP 1354,* pp. 173-195, 2000

3. R.P. MARSHALL, Control of hydride orientation in Zircaloy-4 by fabrication process, *Journal of Nuclear Materials*, **vol. 24**, pp.49-59 (1967)

4. A. RACINE, Influence de l'orientation des hydrures sur les modes de déformation, d'endommagement et de rupture du Zircaloy-4 hydruré, *PhD Thesis Ecole Polytechnique*, 2005

5. H.C. CHU, S.K. WU, R.C. KUO, Hydride reorientation in Zircaloy-4 cladding, *Journal of Nuclear Materials*, **vol. 373**, pp.319-327 (2008)

6. K.W. LEE, S.I. HONG, Zirconium hydrides and their effect on the circumferential mechanical properties of Zr-Sn-Fe-Nb tubes, *Journal of Nuclear Materials*, **vol. 346**, pp.302-307 (2002)

7. R.S. DAUM, S. MAJUMDAR, Y. LIU, M.C. BILLONE, Mechanical Testing of High Burn-up Zircaloy-4 Fuel Cladding under Conditions Relevant to Drying Operations and Dry-Cask Storage, *2005 Water Reactor Fuel Performance Meeting*, Paper 1051, Kyoto (Japan), October 2005

8. T. YELLA REDDY, SR. REID, Phenomena associated with the crushing of metal tubes between rigid plates, *International Journal Solid Structures*, **vol. 16**, pp.545-562 (1980)

9. M. AVALLE, L. GOGLIO, Static lateral compression of aluminum tubes: strain gauge measurements and discussion of theoretical models, *Journal of Strains Analysis*, **vol. 32**, pp.335-343 (1997)

10. V. BUSSER, M.C. BAIETTO-DUBOURG, J. DESQUINES, C. DURIEZ, J.P. MARDON, Mechanical response of oxidized Zircaloy-4 cladding material submitted to a ring compression test, *Journal of Nuclear Materials*, **vol. 384**, pp.87-95 (2009)

11. J.B. BAI, N. JI, D. GILBON, Hydride embrittlement in Zircaloy-4 plates. Part II : Interaction between the tensile stress and hydride morphology, *Metallurgical and Materials Transactions A,* **vol.25***, pp.1199-1208 (1994)*

12. A. ALAM, C. HELLWIG, Cladding Tube Deformation Test for Stress Reorientation of Hydrides, *15th International Symposium on Zirconium in the Nuclear Industry,* Sunriver, Oregon, 2007

13. J.S. BRADBROOK, G.W. LORIMER, N. RIDLEY, The precipitation of zirconium hydride in zirconium and Zircaloy-2, *Journal of Nuclear Materials*, **vol. 42**, pp.142-160 (1972)